

**Dynamical fission in  $^{124}\text{Sn} + ^{64}\text{Ni}$  collision at 35A MeV**

E. De Filippo,<sup>1</sup> A. Pagano,<sup>1</sup> E. Piasecki,<sup>2,\*</sup> F. Amorini,<sup>3</sup> A. Anzalone,<sup>3</sup> L. Auditore,<sup>4</sup> V. Baran,<sup>3</sup> I. Berceanu,<sup>5</sup> J. Blicharska,<sup>6</sup> J. Brzychczyk,<sup>7</sup> A. Bonasera,<sup>3</sup> B. Borderie,<sup>8</sup> R. Bougault,<sup>9</sup> M. Bruno,<sup>10</sup> G. Cardella,<sup>1</sup> S. Cavallaro,<sup>3</sup> M. B. Chatterjee,<sup>11</sup> A. Chbihi,<sup>12</sup> M. Colonna,<sup>3</sup> M. D'Agostino,<sup>10</sup> R. Dayras,<sup>13</sup> M. Di Toro,<sup>3</sup> J. Frankland,<sup>12</sup> E. Galichet,<sup>8</sup> W. Gawlikowicz,<sup>7</sup> E. Geraci,<sup>10</sup> F. Giustolisi,<sup>3</sup> A. Grzeszczuk,<sup>6</sup> P. Guazzoni,<sup>14</sup> D. Guinet,<sup>15</sup> M. Iacono-Manno,<sup>3</sup> S. Kowalski,<sup>6</sup> E. La Guidara,<sup>3</sup> G. Langanó,<sup>1</sup> G. Lanzalone,<sup>3</sup> N. Le Neindre,<sup>8</sup> S. Li,<sup>16</sup> S. Lo Nigro,<sup>14</sup> C. Maiolino,<sup>3</sup> Z. Majka,<sup>7</sup> M. Papa,<sup>1</sup> M. Petrovici,<sup>5</sup> S. Pirrone,<sup>1</sup> R. Płaneta,<sup>7</sup> G. Politi,<sup>1</sup> A. Pop,<sup>5</sup> F. Porto,<sup>3</sup> M. F. Rivet,<sup>8</sup> E. Rosato,<sup>17</sup> F. Rizzo,<sup>3</sup> S. Russo,<sup>14</sup> P. Russotto,<sup>3</sup> M. Sassi,<sup>14</sup> K. Schmidt,<sup>6</sup> K. Siwek-Wilczyńska,<sup>2</sup> I. Skwira,<sup>2</sup> M. L. Sperduto,<sup>3</sup> J. C. Steckmeyer,<sup>9</sup> Ł. Świdorski,<sup>2</sup> A. Trifirò,<sup>4</sup> M. Trimarchi,<sup>4</sup> G. Vannini,<sup>10</sup> M. Vigilante,<sup>17</sup> J. P. Wieleczko,<sup>12</sup> J. Wilczyński,<sup>18</sup> H. Wu,<sup>16</sup> Z. Xiao,<sup>16</sup> L. Zetta,<sup>14</sup> and W. Zipper<sup>6</sup>

(REVERSE Collaboration)

<sup>1</sup>*INFN, Sezione di Catania and Dipartimento di Fisica e Astronomia, Università di Catania, Italy*<sup>2</sup>*Institute of Experimental Physics, Warsaw University, Warsaw, Poland*<sup>3</sup>*INFN, Laboratori Nazionali del Sud and Dipartimento di Fisica e Astronomia, Università di Catania, Italy*<sup>4</sup>*INFN, Gruppo Collegato di Messina and Dipartimento di Fisica, Università di Messina, Italy*<sup>5</sup>*Institute for Physics and Nuclear Engineering, Bucharest, Romania*<sup>6</sup>*Institute of Physics, University of Silesia, Katowice, Poland*<sup>7</sup>*M. Smoluchowski Institute of Physics, Jagellonian University, Cracow, Poland*<sup>8</sup>*Institute de Physique Nucléaire, IN2P3-CNRS, and Université Paris-Sud, Orsay, France*<sup>9</sup>*LPC, ENSI Caen and Université de Caen, France*<sup>10</sup>*INFN, Sezione di Bologna and Dipartimento di Fisica, Università di Bologna, Italy*<sup>11</sup>*Saha Institute of Nuclear Physics, Kolkata, India*<sup>12</sup>*GANIL, CEA, IN2P3-CNRS, Caen, France*<sup>13</sup>*DAPNIA/SPhN, CEA-Saclay, France*<sup>14</sup>*INFN, Sezione di Milano and Dipartimento di Fisica, Università di Milano, Italy*<sup>15</sup>*IPN, IN2P3-CNRS and Université Claude Bernard, Lyon, France*<sup>16</sup>*Institute of Modern Physics, Lanzhou, China*<sup>17</sup>*INFN, Sezione Napoli and Dipartimento di Fisica, Università di Napoli, Italy*<sup>18</sup>*A. Soltan Institute for Nuclear Studies, Swierk/Warsaw, Poland*

(Received 11 March 2005; published 23 June 2005)

Some properties of fast, nonequilibrium splitting of projectiles in the  $^{124}\text{Sn} + ^{64}\text{Ni}$  reaction at 35A MeV were determined using the  $4\pi$  CHIMERA detector system. In particular the charge distributions, in- and out-of-plane angular distributions, and relative velocities of projectilelike fragments were measured. The time scale of the process was estimated and it turned out that the process is sequential but much faster than the ordinary, equilibrated fission.

DOI: 10.1103/PhysRevC.71.064604

PACS number(s): 25.70.Jj, 25.70.Mn, 25.70.Pq

**I. INTRODUCTION**

The phenomenon of fast, nonequilibrium fission of projectilelike fragments (PLF) was first observed in heavy-ion deep-inelastic collisions at rather low energies [1,2], but later it was observed also at higher energies [3,4]. However, it is not clear whether the physics in both cases is the same.

In the case of the equilibrium PLF fission, the angular distribution should be forward/backward symmetric in the PLF reference system. The main signature of nonequilibrium fission is that the heavier of the two fission fragments is usually the faster one (i.e., it is forward directed). Thus, the lighter fragment is situated preferentially between its heavier partner and the targetlike nucleus. In the case of the lightest fragments, we usually characterize this process as midvelocity emission [5] or neck fragmentation [6,7]. Since we do not know whether the reaction mechanism is the same for all

heavy/light fragment mass ratios ( $A_H/A_L$ ), in this paper we provisionally reserve the name “dynamical fission” (DF) for less mass-asymmetric PLF splitting, when  $A_H/A_L < 4.6$ . In our system, for the PLFs of  $Z \approx 50$ , this corresponds to the charge of the lighter DF fragment  $Z_L > 9$ .

In this article we present experimental data obtained in the  $^{124}\text{Sn} + ^{64}\text{Ni}$  reaction, investigated at the laboratory energy  $E_{\text{lab}}(^{124}\text{Sn}) = 35\text{A MeV}$  by using the multidetector CHIMERA, installed at Laboratori Nazionali del Sud (Catania) in 2000 [8]. The experiment was carried out as a part of the so-called REVERSE campaign, in which nucleus-nucleus collisions were studied in reverse kinematics to disentangle dynamical and statistical decays of excited nuclear systems. The reverse kinematics was chosen for easier identification of fragments and emitting sources. The choice of the medium-mass  $^{124}\text{Sn}$  projectile was dictated by research goals of the whole REVERSE campaign. Results obtained for the neutron-poor system  $^{112}\text{Sn} + ^{58}\text{Ni}$ , studied simultaneously in the campaign, are under analysis and will be published later.

\*Electronic address: piasecki@fuw.edu.pl

## II. EXPERIMENT

The CHIMERA detector consists of 1192 two-element telescopes, covering the angular range between  $1^\circ$  and  $176^\circ$  in  $4\pi$  configuration. Each telescope consists of a Si  $300\ \mu\text{m}$ -thick planar detector ( $220\ \mu\text{m}$  at the smallest angles) followed by a CsI(Tl) scintillator detector of thickness ranging from 3 to 12 cm, depending on the detection angle. The REVERSE campaign used only the forward part of the CHIMERA detector, which consists of 688 telescopes covering the angular range between  $1^\circ$  and  $30^\circ$  azimuthally arranged around the beam axis.

The  $^{124}\text{Sn}$  beam with intensity of about  $5 \times 10^7$  particles/s bombarded a self-supporting target of thickness approximately  $310\ \mu\text{g}/\text{cm}^2$ . The data were collected by triggering the data acquisition system in exclusive mode, requiring a silicon multiplicity condition  $\geq 3$ . Three different identification techniques were simultaneously used. The  $\Delta E - E$  technique was employed for charge identification of heavy ions. A good identification of the atomic number (up to the beam charge for the most forward angles) was obtained in 95% of telescopes in the full dynamical range of the experiment, with typical charge resolution as good as  $\delta Z/Z \sim 1.2\%$  (FWHM) in the region of atomic number  $Z = 50$ . Isotopic identification of light ions ( $Z < 10$ ) at larger angles ( $\Theta > 10^\circ$ ) was achieved by the  $\Delta E - E$  method too.

The time-of-flight measurement (TOF), using the high-frequency signal from the superconducting cyclotron as reference and the timing signal from the Si detectors as the start time for the time to digital converter, allowed velocity measurements of ions with  $Z > 2$ . The good timing performance of the LNS superconducting cyclotron pulsed beam allowed us to achieve a typical time resolution of  $\delta t \sim 0.8\ \text{ns}$  (FWHM). The TOF together with energy left in the  $\Delta E$  silicon detector was also employed for mass identification of the low-energy light fragments ( $Z < 15$ ) stopped in the Si detector. A pulse shape analysis method was used for the isotopic identification of energetic light charged particles, which were stopped in the scintillator. Some experimental details can be found in Ref. [9].

Linearity of electronic chains as good as 0.3% was measured and monitored by special short runs with a precision pulse generator spanning the full range of the CHIMERA charge to digital converters. The typical energy resolution of CHIMERA telescopes was  $\delta E/E < 1\%$  (FWHM) for the Si detectors (as measured with elastic scattering), about 70 keV with the  $\alpha$  source, and about 2% for the CsI(Tl) scintillator as evaluated by elastic scattering. To reduce possible distortions of the electric field, the polarization bias of the Si detectors was increased by 30% with respect to the nominal one.

Energy calibrations and energy resolution evaluations were performed using elastic scattering of light (i.e.,  $^{12}\text{C}$ ,  $^{16}\text{O}$ , and  $^{19}\text{F}$  around 5A MeV) and heavy-ion beams (i.e.,  $^{58,60}\text{Ni}$  and  $^{112,124}\text{Sn}$  around 15A MeV), delivered by the tandem and the cyclotron, and a standard mixed nuclide radioactive  $\alpha$  source ( $^{239}\text{Pu} + ^{241}\text{Am} + ^{244}\text{Cm}$ ).

The TOF calibration was performed by evaluation of the time offset  $t_o$  [10] for each individual detector by a fitting procedure for well-defined loci (corresponding to mass numbers

$A = 7, 11,$  and  $15$ ) in the energy versus TOF identification matrix. The desired behavior of the  $t_o$  parameter, namely, independence of particle mass and energy, was obtained only for ion energies corresponding to punching through particles, for kinetic energy above 12A MeV. In the case of the particles stopped in the detectors, use was made of an iterative method [11], that took into account the pulse shape effects in the constant fraction discriminators.

## III. DATA ANALYSIS AND RESULTS

Since we are interested in fission of the projectilelike fragments in semiperipheral collisions, we concentrate our attention on the two heaviest fragments accompanied by at most four other charged fragments, so the total charged particle multiplicity condition set in off-line analysis was  $M_{\text{tot}} < 7$ . The forward part of CHIMERA, having close to 100% detection efficiency of PLF, has much lower efficiency for targetlike fragments (TLF); thus to keep statistics as high as possible, in data analysis we did not impose the condition of recording in coincidence the PLF and TLF. Consequently, we did not apply the usual condition of (almost) complete fragment charge and momentum detection. Instead, we have selected  $8.5 \times 10^6$  events fulfilling the condition of total recorded charge  $30 < Z_{\text{tot}} < 80$  and of the sum of charges of the two heaviest fragments  $Z_{2F} > 15$ . Additional conditions concerning the kinetic energy loss in the collision as well as the assumed source of the fragments and their mass range were applied. These are explained in the following sections.

### A. Sources

We selected here the events corresponding to the mass ratio of the two heaviest fragments  $A_H/A_L < 4.6$  because of our interest in the dynamical fission of PLF. The distribution (on a logarithmic scale) of the number of counts as a function of  $Z_{2F}$  and the parallel velocity (in the laboratory reference frame) of the lighter of the two fragments,  $V_{\text{par}}^L$ , is presented in Fig. 1 for three mass asymmetries  $A_H/A_L$  and for three ranges of the total kinetic energy of the two heaviest fragments,  $E_{2F}$ . This latter quantity is related to the total kinetic energy loss (and centrality of collision), being however easily accessible in our measurements, whereas determination of the *total* kinetic energy loss requires complete recording and reconstruction of events. One should stress, however, that  $E_{2F}$  is not directly connected with the energy dissipation: A change of  $E_{2F}$  by 46% (from 3800 to 2600 MeV) is correlated with rather modest slowing down of the fragment source (by some 7%). Thus, at this beam energy, the majority of the energy loss is caused by the loss of fragment mass owing to emission of light fragments and neutrons. Nevertheless, the microscopic transport model calculations [7] show that  $E_{2F}$  can be used as a measure of impact parameter during the collision step of the reaction.

The same kind of plots, for the heaviest fragment shows that its velocity ( $V_{\text{par}}^H$ ) was always close to the beam velocity (which is why we present the results for lighter fragments only). However, for the lighter (of the two heaviest) fragments we see that their velocities have broad distributions consisting

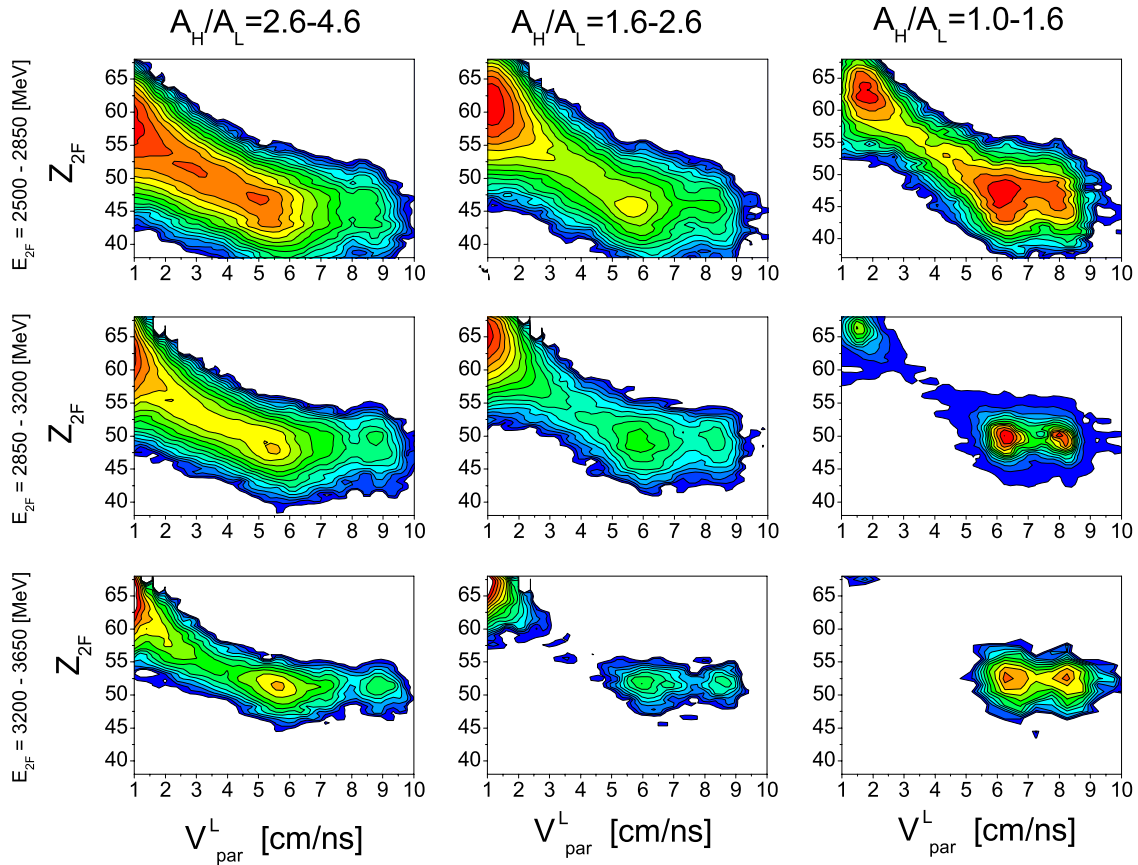


FIG. 1. (Color online) The sum of charges of the two heaviest fragments ( $Z_{2F}$ ) vs the lighter fragment parallel velocity (in the laboratory reference frame) for different mass asymmetries and different ranges of kinetic energy of these two fragments. The distributions are shown on a logarithmic scale; the red color corresponds to the highest cross section. The beam velocity was equal to 8.2 cm/ns.

basically of two main components: one of very low velocity (about 1 cm/ns) and the second one close to the beam velocity. It is striking that the low-velocity group comes from the events in which  $Z_{2F}$  is higher than the  $Z$  of the projectile. However, one can easily check that they cannot be related to fusion (complete or incomplete) followed by fission, because the products of such a process should have higher velocities ( $V_{par}^L > 5$  cm/ns). Low-velocity fragments can be interpreted as target remnants, as suggested by simple kinematical calculations and in agreement with model calculations [7]. This interpretation agrees also with the conclusion of the analysis of the same data made under condition of coincidence of the three heaviest fragments [12].

On the other hand, the fact that the high-energy group has  $Z_{2F}$  close to about 45–50 suggests that for  $V_{par}^L > 4$  cm/ns we observe essentially splitting of the PLF into two main fragments. This is also reported by Refs. [7,12,13].

This information is important for the interpretation of  $V_{per}^L$  versus  $V_{par}^L$  (perpendicular versus parallel component of velocity) plots, shown in Fig. 2, after putting an additional condition on  $Z_{2F}$ , corresponding to PLF. Since the maximum  $Z_{2F}$  of the high-velocity group shifts downward for smaller  $E_{2F}$  (see Fig. 1), we changed also slightly the upper limits of the  $Z_{2F}$  windows, shown on the left side of Fig. 2. In Fig. 2 we see structures reminiscent of Coulomb rings,

centered somewhat below the beam velocity of  $V_{beam} = 8.2$  cm/s. The rings point to a well defined PLF source and make probable the scenario of two separate (sequential) reaction steps: scattering of the PLF followed by their splitting into two fragments. Moreover, we see that the light fragments most frequently occupy the low-velocity sides of the rings. This is the signature of “dynamical fission,” namely, the fact that the lighter fragments are emitted preferentially backward in the PLF reference system (i.e., toward the target nucleus). The lack of forward/backward symmetry of the rings shows that the second step is a very fast process, with the time interval between the two steps much shorter than the PLF rotation time; otherwise the averaging over the emission directions would result in forward/backward symmetry. This is why we consider this process as being the “fast sequential” one. In addition, at somewhat lower (intermediate) velocity, outside of the rings, we see also light fragments not forming any ringlike structures. They are described in Ref. [7] as the “neck emission.” The novel experimental method of time-scale determination of these fragments’ production is discussed in [13].

It is seen that for the near-symmetric splits the fragments sequentially emitted from PLF dominate over the mid-velocity particles, even if this dominance gradually decreases with increased mass asymmetry and with kinetic energy loss in the collision step.

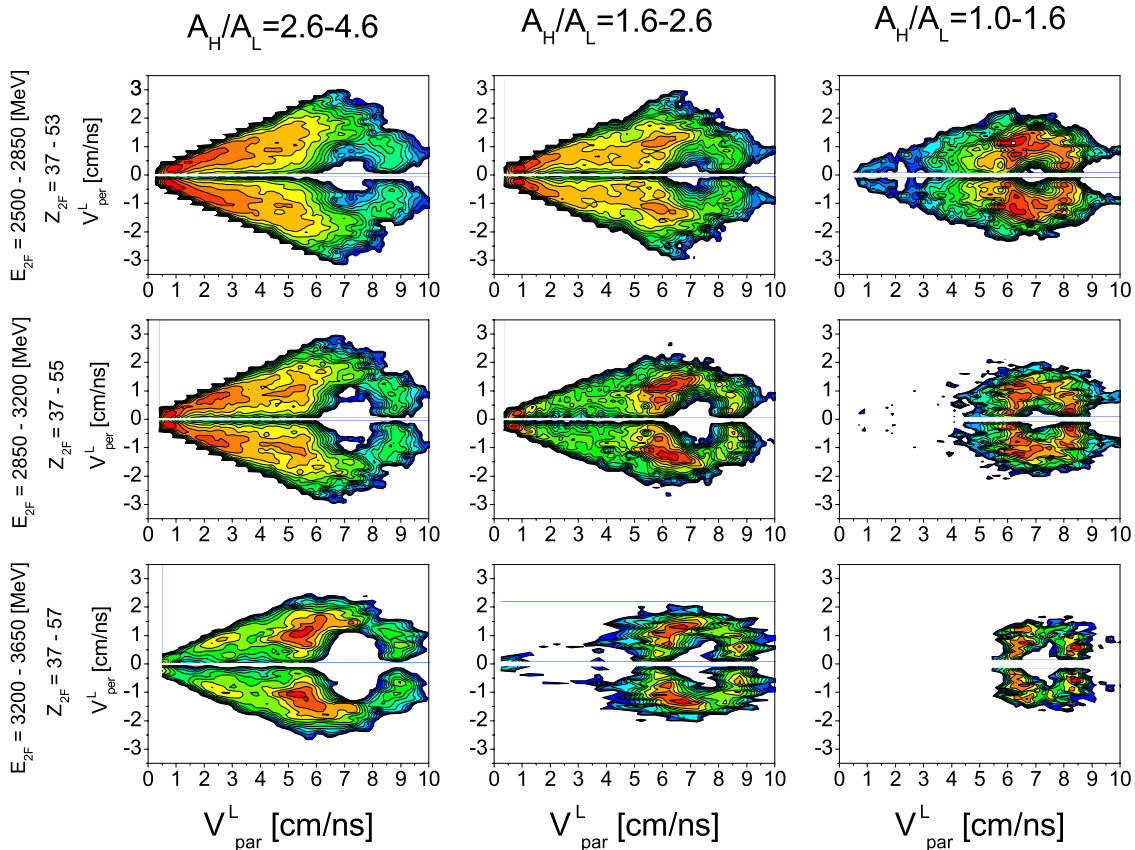


FIG. 2. (Color online)  $V_{\text{per}}^L$  vs  $V_{\text{par}}^L$  plots for the lighter fragment (of the two heaviest) for different values of mass asymmetry and kinetic energy of these fragments. The sharp cuts in the region of  $V_{\text{par}}^L < 5$  cm/ns are due to the angular range of the forward part of CHIMERA being limited to  $30^\circ$ . The distributions are shown on a logarithmic scale; the red color corresponds to the highest cross section.

### B. Charge distribution

To get rid of the TLF we should put a condition on  $V_{\text{par}}^L$ . This is a delicate point. According to [7,12] a value of 3 cm/ns would be quite safe. For the very symmetric splits (the rightmost column of Fig. 2) any value between 3 and 5 cm/ns would be acceptable. However, for more asymmetric splits, especially for smaller  $E_{2F}$ , we observe more and more of the intermediate-velocity fragments (IVF), and their number becomes comparable with those accumulating on the Coulomb rings. Moreover, for higher asymmetry, because of momentum conservation, the Coulomb rings become larger and the condition  $V_{\text{par}}^L > 5$  cm/ns would cut out part of them. Thus our choice should depend on a decision of how large a contribution of the IVF we are ready to tolerate in the study of DF. To compare our data to the “neck emission” products, which in our system, according to the Boltzmann-Nordheim-Vlasov (BNV) transport calculations [7], appear mainly in the interval 3.5–5 cm/ns, we have chosen the compromise condition  $V_{\text{par}}^L > 4$  cm/ns, realizing, however, that for asymmetric splits any such crude condition would result in some distortion of results.

The conditions  $M_{\text{tot}} < 7$ ,  $E_{2F} > 2500$  MeV,  $Z_{2F} = 37$ –57, and  $V_{\text{par}}^L > 4$  cm/ns are satisfied by 13% of all recorded events, but in most cases the splitting is very asymmetric (i.e., the lighter fragment is very light indeed). This is shown in Fig. 3 for three ranges of kinetic energy loss. However, one can see

that nearly symmetric PLF splitting ( $Z_L \geq 20$ –23) represents still quite a sizable part of this sample, especially for less peripheral collisions ( $E_{2F} = 2500$ –2850 MeV).

According to the BNV calculations, the energy range  $E_{2F} = 2500$ –3200 MeV corresponds to the impact parameter range  $b = 6$ –8 fm (where contributions from each impact parameter were summed with the corresponding geometrical weight). The slope of the calculated distribution, obtained in Ref. [7], roughly filtered by the REVERSE-CHIMERA geometry (acceptance in the range  $1^\circ$ – $30^\circ$ ), seems to be larger than that of the experimental one, although one should emphasize that because of low statistics theoretical predictions are limited to  $Z_L < 12$ .

### C. Angular distributions

We define the reaction plane by the beam and the velocity vector of the scattered PLF. The latter is reconstructed from the velocity vectors of the two heaviest fragments for events fulfilling the selection conditions given previously. The definition of the in-plane angle  $\Phi_{\text{plane}}$  and out-of-plane angle  $\Psi_{\text{out}}$  can be seen in Fig. 4. The precise way of calculating the angles, using the fragment-velocity vectors, is given in Ref. [2]. The results of such an analysis for various kinetic energy losses and mass asymmetries are presented in Figs. 5 and 6 and are described in the following.

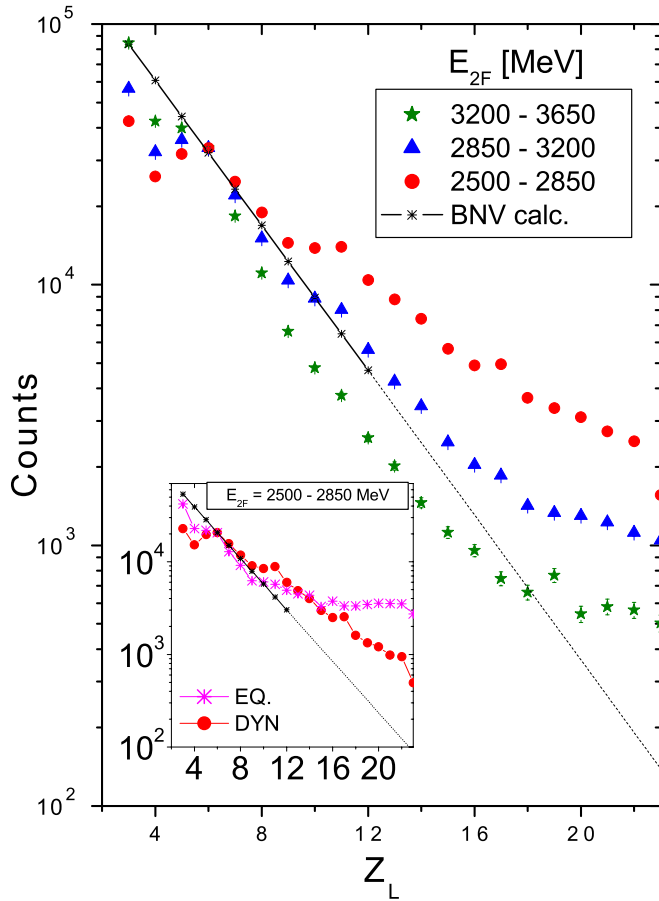


FIG. 3. (Color online) Atomic number distributions of the lighter (of two heaviest) fragments of the PLF splitting, arbitrarily normalized at  $Z_L = 6$ . The theoretical distribution is calculated for  $E_{2F} = 2500\text{--}3200$  MeV. Because of low statistics the distribution is limited to  $Z_L \leq 12$ ; results for higher  $Z_L$  are extrapolated (dotted line). The inset shows comparison of slopes of the “equilibrated” and “dynamical” processes (see Sec. III C1).

### 1. In-plane distributions

The direction  $\Phi_{\text{plane}} = 0^\circ$  in Figs. 4 and 5 corresponds to the heavier fragment moving forward, strictly along the PLF flight direction; according to the sign convention chosen in Ref. [2], positive  $\Phi_{\text{plane}}$  values mean that the fragment is deflected toward the beam direction.

The slow (equilibrated) fission, because of memory loss after many PLF rotations, should result in a flat in-plane distribution [2]. We see, however, distinct maxima in the distributions, located close to  $0^\circ$ , being a manifestation of dynamical fission.

For moderately mass-asymmetric divisions ( $A_H/A_L = 2.6\text{--}4.6$ ) the maximum dominates the flat equilibrated component, indicated by the straight line in Fig. 5, but also for smaller mass asymmetries the maximum, even if weaker, is still distinct. This clearly points to nonequilibrium dynamical fission processes: The existence of the maximum means that the process is fast, otherwise one would observe the averaged-out flat angular distribution.

The observed right–left asymmetry of the  $\Phi_{\text{plane}}$  distribution around  $0^\circ$  is also of interest as a clear indication of the dynamical properties of the process. There are at least two sources of the asymmetry: the angular momentum acquired during the collision and the mass (charge) asymmetry in the entrance channel, giving rise to the strong Coulomb repulsion. The first effect results in the PLF rotation before its splitting and the fragment (orbital) rotation after it. The second effect was predicted and discussed in the context of neck fragmentation in Ref. [7].

The determined distributions are to some extent disturbed by two effects: the choice of the  $V_{\text{par}}^L$  selection condition (discussed previously) and the imperfections of the detection system. The detection efficiency of the detector system depends on the phenomenon under study. Unfortunately, presently there is no model that describes well dynamical fission (for this range of fragment mass asymmetry) so we could not pass theoretical results through the experimental filter. In this situation we performed simulations of the CHIMERA detection efficiency by using an event generator and assuming statistical fission of PLF after scattering on the target (see Appendix). Dependence of efficiency on the source velocity, scattering angle, fission asymmetry, in- and out-of-plane angles, and relative fragment velocity, some of which are different in equilibrium and dynamical fission, were taken into account. We concluded that the efficiency dependence on  $\Phi_{\text{plane}}$  is pretty flat (and close to 100%) apart from the dips in the in-plane distribution close to  $\pm 15^\circ$  and  $\pm 165^\circ$ , caused by the beam exit hole of the detector system. For the mass asymmetry  $A_H/A_L < 2.6$  this is the main reason for the distortions of maxima seen in Fig. 5. For larger asymmetry, especially for large kinetic energy loss, a more important

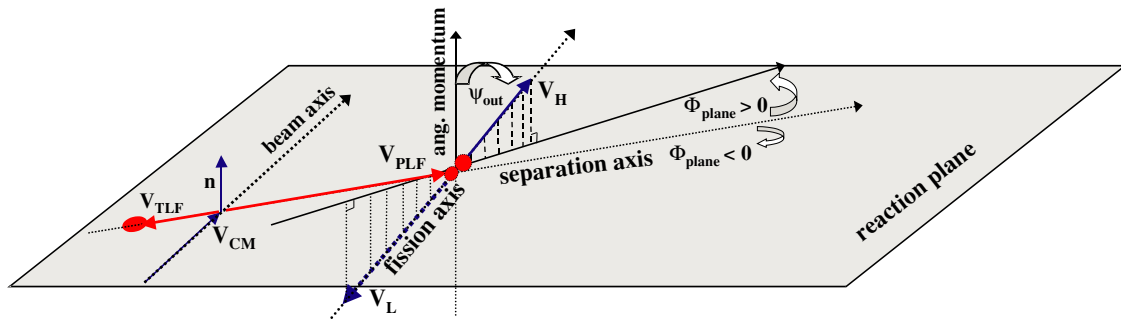


FIG. 4. (Color online) Diagram indicating the definition of the in-plane ( $\Phi_{\text{plane}}$ ) and out-of-plane ( $\Psi_{\text{out}}$ ) angles.

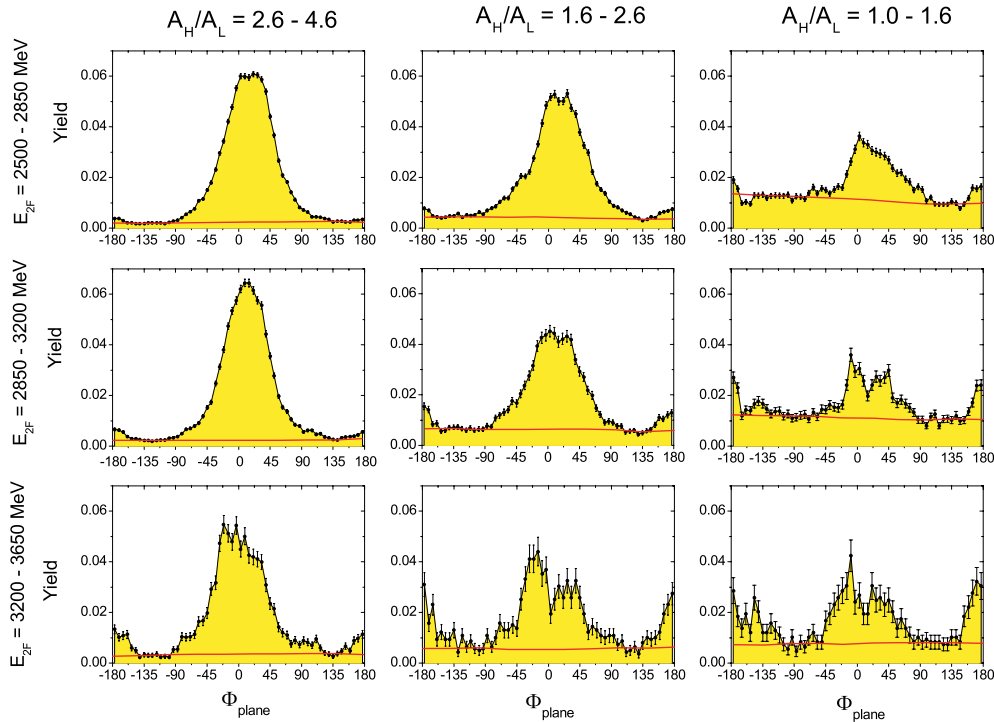


FIG. 5. (Color online) Normalized to unity in-plane angular distributions of the heavier fragment from the PLF splitting. Zero degrees corresponds to forward emission; positive angles correspond to deflection of the fragment toward the beam. Note the presence of a second maximum (at  $\pm 180^\circ$ ), corresponding to the forward emission of the lighter fragment. The straight line, corresponding to the equilibrated component, was used for calculation of results presented in Table I.

uncertainty of the peak shape comes from the somewhat arbitrary value of the  $V_{\text{par}}^L$  condition and, more generally, from difficulties of distinguishing between the IVF and DF events. It is difficult to say precisely to what extent this part of the angular distribution is depleted by both these effects, but we estimate that, depending on asymmetry and kinetic energy loss, it is limited to 15–30%.

However, since equilibrated (EQ) fission should result in a flat in-plane distribution, its contribution is easy to calculate and in this way we could estimate *lower limits* of the dynamical (DYN) component (see Table I) as a function of  $E_{2F}$  and splitting asymmetries.

If one takes into account the estimated depletion of the DF peak, the previous percentage increases by a few percent.

Further, we can compare properties of the dynamical and equilibrated processes, choosing the appropriate regions of  $\Phi_{\text{plane}}$ , dominated respectively by DYN ( $-30^\circ < \Phi_{\text{plane}} < 45^\circ$ ) and EQ components ( $-130^\circ < \Phi_{\text{plane}} < -90^\circ$  and  $90^\circ <$

TABLE I. Lower limits of DF percentage defined as 100·DYN/(DYN + EQ).

$E_{2F}$ [MeV]	$A_H/A_L$		
	1.0–1.6	1.6–2.6	2.6–4.6
3200–3650	52	65	80
2850–3200	31	63	87
2500–2850	32	76	87

$\Phi_{\text{plane}} < 130^\circ$ ), even if this differentiation is not perfect. In particular, in the inset to Fig. 3 we compare the (arbitrarily normalized at  $Z_L = 6$ ) charge distributions for these components. It is seen that for  $Z_L > 12$  the EQ distribution stays essentially flat, whereas the dynamical one decreases exponentially. The flat shape results from the PLF being close to the Businaro-Gallone point [2]. That the distribution for the dynamical component is different simply means that the role of the potential energy surface is not dominant here, in contrast to the case of equilibrated fission.

Note that in our case, because of dominance of dynamical fission, the total distribution is exponential. We checked that the same stays true after transformation from  $Z_L$  to asymmetry parameter  $\eta = (A_H - A_L)/(A_H + A_L)$ , used in Ref. [2], where the reaction  $^{120}\text{Sn} + ^{120}\text{Sn}$  at 18.4A MeV has been studied. This is in clear disagreement with their result: The flat asymmetry distribution in the range  $\eta = 0-0.5$  (corresponding to  $Z_L > 14$ ) was observed even without separation of the EQ and DYN components. The probable reason of this difference is the lower beam energy used in their experiment, which resulted in a much smaller contribution of the dynamical fission.

## 2. Out-of-plane distributions

The out-of-plane angle is usually defined as an angle with respect to the normal to the reaction plane (see, e.g., Ref. [14]). Thus  $\Psi_{\text{out}} = 90^\circ$  corresponds to in-plane emission. We calculated the distributions of  $\Psi_{\text{out}}$  separately for the

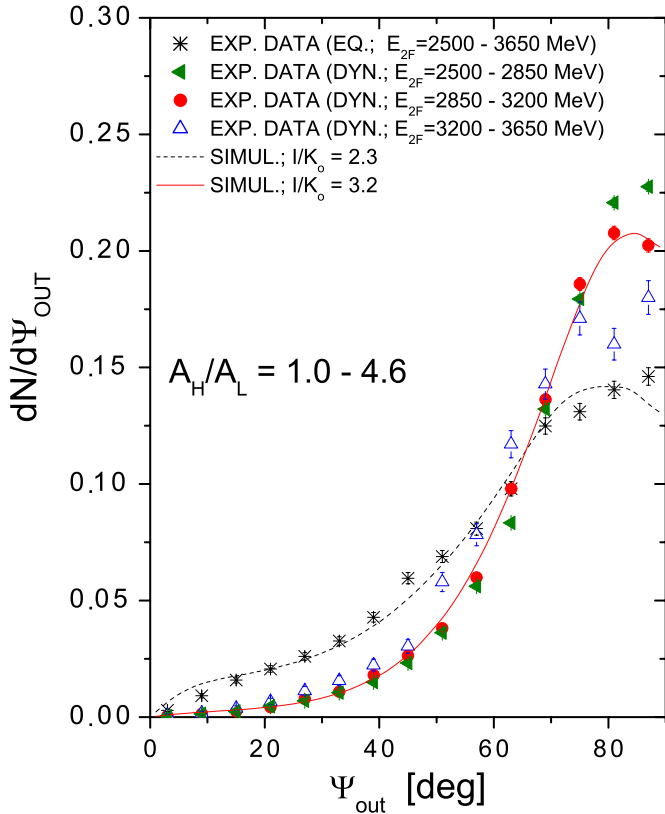


FIG. 6. (Color online) Normalized to unity out-of-plane angular distributions of fission fragments (for  $A_H/A_L = 1.0-4.6$  and for given  $E_{2F}$  intervals), corresponding to the “dynamical” ( $-30^\circ < \Phi_{\text{plane}} < 45^\circ$ ) and “equilibrium” ( $-130^\circ < \Phi_{\text{plane}} < -90^\circ$  and  $90^\circ < \Phi_{\text{plane}} < 130^\circ$ ) angular ranges. Dashed lines show results of the statistical model calculation after it is passed through the experimental filter.

DYN and EQ components. It turned out that the out-of-plane distributions do not depend on the mass asymmetry, so we could construct both (DYN and EQ) distributions by summing the data over the whole asymmetry range  $A_H/A_L = 1.0-4.6$ . However, we checked that although the “equilibrated” part does not depend on the kinetic energy loss, the “dynamical” one depends on it to some extent.

One should remember that in equilibrium fission the width of the out-of-plane angular distribution depends on the angular momentum, moment of inertia, and temperature of the fissioning system [14,15]; thus the observed independence is rather surprising. Nevertheless we can present in Fig. 6 the distribution for the equilibrated component summed over the considered energy range  $E_{2F} = 2500-3650$  MeV, whereas for DF we show the distributions for three energy intervals. According to our simulations, the dependence of the distribution on  $E_{2F}$  is not an artifact and in any case it is clear that the width of the EQ distribution is significantly (by about 70%) larger than that of the DYN ones.

The equilibrated component can be described by the statistical model. The relevant model parameter is  $I/K_o$ , the ratio of the mean angular momentum and the rms width of its projection on the nuclear symmetry axis. The  $K_o$  is given by  $K_o^2 = T\mathfrak{I}_{\text{eff}}/\hbar$ , with  $T$  being the temperature of the

fissioning nucleus at the saddle point and  $\mathfrak{I}_{\text{eff}}$  the effective moment of inertia. After taking into account the resolution and efficiency of CHIMERA, we obtained a good description of the experimental out-of-plane distribution with  $I/K_o = 2.3 \pm 0.1$ . Determining the angular momentum is more difficult as the temperature and moment of inertia can be estimated only roughly. However, it is known from many papers (see, e.g. [15]) that  $K_o$  is usually of the order of 10–12, which would correspond to an angular momentum at the moment of scission of about  $25-30\hbar$ . Taking into account that in the time interval between collision and scission a few  $\hbar$  units are usually taken away by the evaporated light particles, we find that this result agrees quite well with the spin transfer calculated using the quantum transport model (see Sec. V).

#### D. Relative velocities

Next, information on the properties of the DF phenomenon is obtained from analysis of relative velocities of the two heaviest fragments. It turns out that the ringlike structures in the  $V_{\text{per}}^L$  versus  $V_{\text{par}}^L$  plots are not circular but rather reminiscent of ellipses. In Fig. 7 we present the angular distributions of the relative velocity normalized to the velocity resulting from Coulomb repulsion, taken event by event according to the Viola systematics for asymmetric systems [16]. It is seen that the predictions based on this systematics, established for equilibrium fission, agree with our data only for fragments emitted at large angles ( $> \pm 70^\circ$ ), whereas for DF the mean relative velocities become larger by some 10–40% even for  $A_H/A_L$  close to 1.0. Moreover, for the “dynamical” events not only is the most probable velocity higher but also the width of the distribution is larger.

This means that even if it appears to definitely be a sequential process, the velocity field of various parts of the PLF does not attain equilibrium. This effect is weakest for more symmetric splitting, pointing to the longer time scale in this case. The angular dependence of relative fragment velocity was already observed earlier (see, e.g., Ref. [4]), even if it was presented in a different way. However, one should emphasize that the character of this dependence, seen with the lower energy beam [1,17], was qualitatively different, namely, the  $V_{\text{rel}}$  was the smallest for  $\Phi_{\text{plane}} \approx 0^\circ$ . The probable reason is that in the lower energy experiments the modulation of  $V_{\text{rel}}$  as a function of angle is caused by the proximity effect, the influence of the target Coulomb field.

After closer inspection of Fig. 7 one can notice some interesting details, which are not easy to interpret. First, one can see that close to  $\pm 120^\circ$  the normalized relative velocity  $V_{\text{ratio}}$  attains a minimal value, significantly smaller than 1.0, and then rises again. If this is caused by strong deformations, or even oscillations, it is not obvious why it is seen at this particular angle. Second, in more peripheral collisions ( $E_{2F} > 2850$  MeV), for near-symmetric splitting the  $V_{\text{ratio}}$  is very close to 1.0 throughout the entire angular range, even if DF is clearly present (see, Fig. 5). This could mean that for such splits the velocity field gets equilibrated faster than the fragments can be de-aligned. Next, it is worth noticing that for the peaks observed near  $\pm 180^\circ$  in the in-plane angular

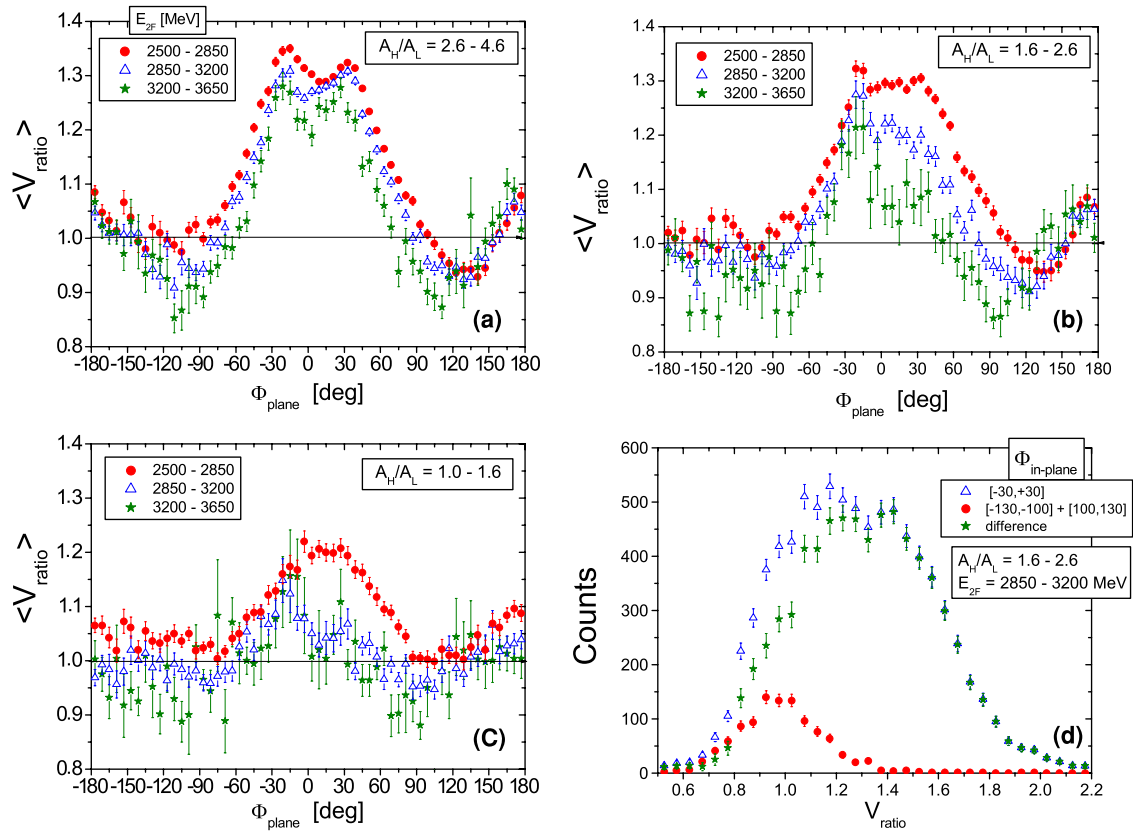


FIG. 7. (Color online) Relative velocity of the PLF normalized by Viola systematics ( $V_{\text{ratio}}$ ). (a), (b), (c) Mean values of the relative velocity as a function of the in-plane angle for different centralities of collision and asymmetries of the PLF splits; (d) example of velocity spectra at the “dynamical” and “equilibrium” angular regions and the resulting net “dynamical” spectrum after subtraction of the background of the “equilibrated” one.

distribution (Fig. 5), the relative fragment velocity is close to that of equilibrated fission, so apparently their (unknown) nature is different from those close to  $0^\circ$ . These peaks are most spectacular for nearly symmetric ( $A_H/A_L = 1.0\text{--}1.6$ ) splitting after most peripheral collisions, where the intensity of these two kinds of nonstatistical splitting is comparable. In fact, solely because of the contribution of the peaks close to  $\pm 180^\circ$ , the percentage of DF, given in Table I, rises in a quite unexpected way for this class of events (i.e., for smallest  $A_H/A_L$  and largest  $E_{2F}$ ).

#### IV. TIME SCALE ESTIMATION

According to the method applied in Ref. [13], the fragments emitted on the shortest time scale ( $t < 100\text{--}150$  fm/c) are visible outside the Coulomb rings. For longer times the fragments “accumulate” on the rings and the method is unable to give time information. For these events we tried to use the method of Ref. [2], which exploited the shift from  $0^\circ$  of the main maximum in the in-plane distribution. It was based on the assumption of rigid body rotation of the PLF and on knowledge of the average angular momentum transferred to the PLF during scattering. According to the BNV calculations, this quantity for semiperipheral collisions is about  $30\hbar$ , being

almost independent of impact parameter. The result is very close to the one determined (also in a model-dependent way) for the equilibrated fission from the out-of-plane angular distribution (see Sec. IV C2). The method applied to our data gave a time interval between PLF scattering and scission of  $12\text{--}120$  fm/c, depending on mass asymmetry and  $E_{2F}$  values. For the most peripheral collisions one gets particularly short times, during which the PLF would have enough time to pass only a few femtometers before splitting. This seems to be an unrealistically short time, given the evidently sequential character of the process, seen in the form of the Coulomb rings, and in comparison with results of the method of time scale estimation based on the relative velocity correlations [13].

The reason for this inconsistency is suggested by the BNV calculations, according to which immediately after collision the PLF are not rotating, being rather frozen in an aligned configuration and all the angular momentum is stored in the dinuclear composite system. The transfer of angular momentum to the PLF will take some time, which is of the order of the freeze-out time corresponding to the centrality of the collision. In fact this roughly gives the time scale of the PLF formation, that is, the time needed for the projectile nucleons to develop all the corresponding collective properties (e.g., mean field and angular momentum). As is shown by the dynamical simulations, the time scale of such “collectivization” is of

the order of 200 fm/c (see in particular Figs. 2–4 of Ref. [7].) According to the model, only after this time do the PLF acquire collective rotation and only from this moment onward does the in-plane peak give some information on rotation (and splitting time) of the PLF. We do not know this delay precisely; thus we can only estimate that the time interval between collision and PLF splitting is in the range 100–300 fm/c. In any case this is a much shorter time scale than that necessary for equilibrated fission, which, according to many experiments, is at least 10–100 times longer [16,18].

It is important to note that for the more symmetric splits almost all fragments form Coulomb rings, whereas the asymmetric cases (very light fragments) also fill the space outside the rings. This means [13] that in the latter case the fragments are produced also on the shorter time scale.

Another argument for the relatively short time scale of sequential dynamical fission can be seen in Fig. 6, where we show the out-of-plane angular distributions, separately for the dynamical and equilibrated components. As one can see, fragments originating from dynamical fission are more concentrated in the reaction plane than those from the equilibrated component. The ratio  $I/K_o$  needed to parametrize the distribution in the former case is 3.2, rather than the 2.3 observed for the equilibrated component.

We do not know whether this difference is caused by larger angular momenta, sampled by DF, or by smaller  $K$  value. It is worth recalling in this context the anomalously large anisotropies of fission fragment angular distributions, observed at much lower energies, interpreted [20] as a result of preequilibrium fission, when the initially narrow distribution of the projection of angular momentum along the symmetry axis has no time to attain its asymptotic, equilibrium value.

## V. DYNAMICAL FISSION AND BNV CALCULATIONS

Some light on the dynamics of these splitting processes could be shed by theoretical predictions within the BNV transport model [7]. The simulations based on this model describe well the “neck emission” in which very light fragments, being the remnant of the neck, are emitted in a very short time ( $t < 120$  fm/c, but with the most probable  $t \approx 25$  fm/c after projectile-target collision [13]), with velocity  $3.5 < V_{\text{par}}^L < 5$  cm/ns [7]. However, the model has problems in predicting the existence of the experimentally observed fragments having larger velocities and forming ringlike structures, demonstrating sequential decay of some well-defined sources. A possible reason is related to the way the fluctuations are included in the model, which are probably not strong enough. It seems that although for neck emission volume instabilities are the most important type, for dynamical fission the shape fluctuations can dominate in conditions for which the velocity fields are not fully equilibrated.

One should stress that the model does predict production of strongly deformed PLF, which might be candidates to undergo DF, having their time scale slowed down with respect to neck fragmentation due to, among others, more symmetric splitting. Unfortunately, because of numerical difficulties, further dynamical evolution of the stretched PLF cannot be

traced in the present form of the BNV model, so it is difficult to say how many fragments will finally fission. There are, however, some arguments supporting the idea that DF (i.e., fast sequential PLF splitting) is essentially of the same nature as that described as neck fragmentation. Among these arguments are the clear alignment signature, the similarity of deviations from the Viola systematics, and the similarity of the charge distributions.

A stimulating picture is emerging for the possibility of studying a continuous transition from the neck fragments, produced at midrapidity via bulk instabilities, to the fast fission fragments produced at the projectile (target) rapidity via shape instabilities. We already observe a hierarchy of the corresponding time scales and we can speculate that the “statistical fission” represents a limiting case of such a transition, on a very long time scale.

## VI. SUMMARY

We studied the  $^{124}\text{Sn} + ^{64}\text{Ni}$  reaction at 35A MeV incident energy. Out of all registered events, about 13% fulfilled the condition of observing the PLF splitting into two main fragments after midperipheral collision ( $Z_{2F} = 37\text{--}57$ ,  $M_{\text{tot}} < 7$ ,  $E_{2F} > 2500$  MeV). The more asymmetric splittings, giving rise to very light fragments, are well described as neck fragmentation, occurring almost immediately after collision ( $t < 120$  fm/c [7,13]). However, in about 20% of cases fulfilling the conditions given, the PLF split in comparable fragments ( $A_H/A_L < 4.6$ ). This class of events is dominated by a clearly sequential process: fission after collision. In at least 35–90% of cases, depending on kinetic energy loss in the collision and on the splitting asymmetry, in a relatively short time after collision ( $100 < t < 300$  fm/c) PLF undergo dynamical fission into two aligned fragments; in the remaining cases we observe typical equilibrium fission, known to be slower by one or two orders of magnitude. The nonequilibrium properties of the DF are reflected in the in- and out-of-plane angular distributions, as well as in the relative velocities of fragments. The charge distribution of DF fragments is apparently also different from the equilibrated fission ones. The contribution of DF (in comparison with equilibrated fission), being rather weakly dependent on kinetic energy loss during the collision stage, increases with mass asymmetry but is still significant even for almost symmetric splitting.

## ACKNOWLEDGMENTS

We are grateful to R. Bassini, C. Boiano, C. Calí, R. Cavaletti, V. Campagna, O. Conti, M. D’Andrea, A. Di Stefano, F. Fichera, N. Giudice, A. Grimaldi, N. Guardone, H. Hong, P. Litrico, S. Marino, D. Moisa, D. Nicotra, G. Peirong, R. Rapicavoli, G. Rizza, S. Salomone, G. Saccà, V. Simion, and S. Urso for their invaluable help in assembling the forward part of CHIMERA. Thanks are due to C. Marchetta and C. Costa for preparing high-quality targets and also to D. Rifuggiato, L. Calabretta, and their coworkers for

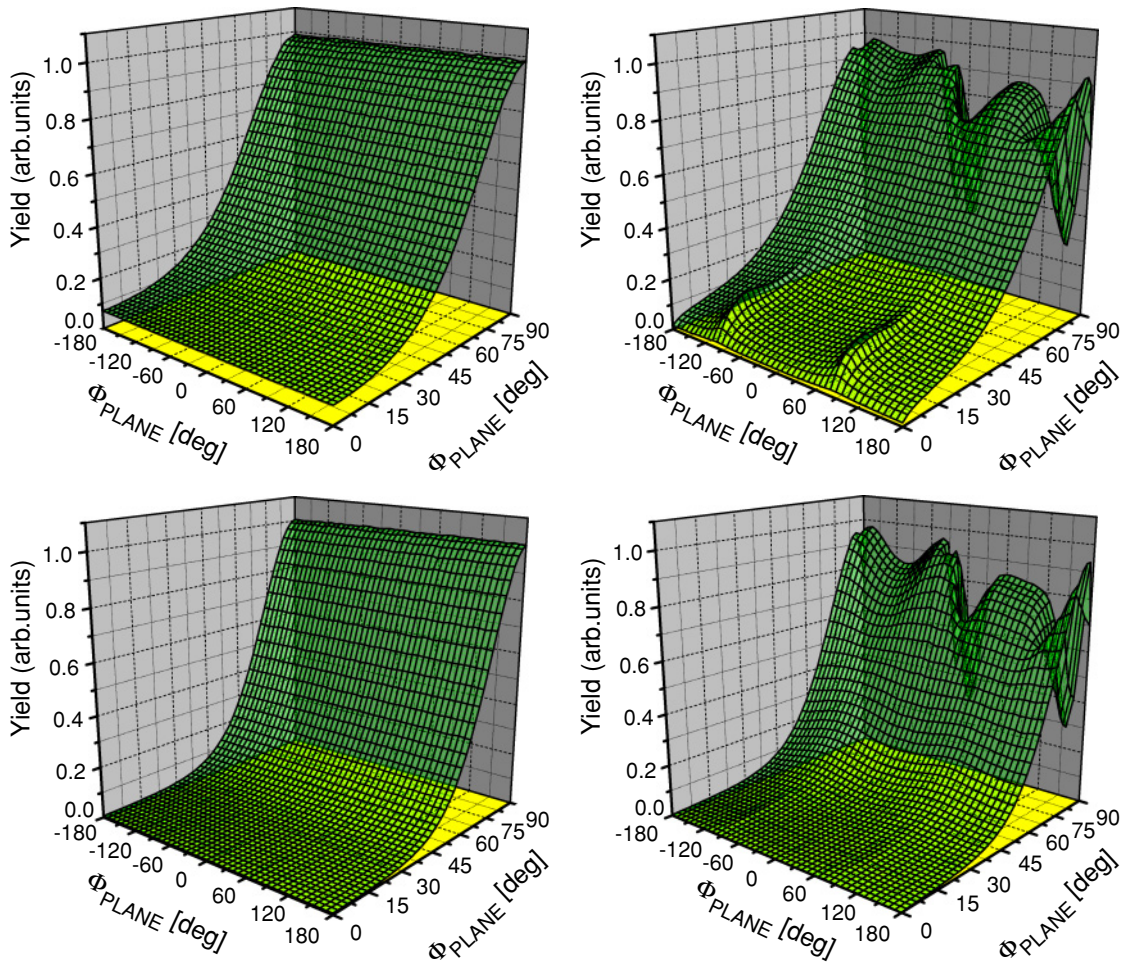


FIG. 8. (Color online) Simulation of the response of the CHIMERA system for the  $\Phi_{\text{plane}} - \Psi_{\text{out}}$  distributions. The left figures show distributions generated for equilibrated (upper figures) and dynamical (lower figure) components of PLF fission (the  $\Phi_{\text{plane}}$  distributions are assumed flat in both cases). The right figures show modifications of these distribution by imperfections and the angular resolution of the detection system.

delivering beams of perfect time characteristics. This work was supported in part by the Italian Ministero dell'Istruzione, dell'Università e della Ricerca (MIUR) under Contract No. COFIN2002 and by NATO Grant No. PST.CLG.079417.

#### APPENDIX: SIMULATIONS OF SOME CHIMERA MEASUREMENT CHARACTERISTICS

The quality of a detector system depends both on the instrument characteristics and on the phenomenon under study. We are interested here in the quality of recording in coincidence two fragments of PLF fission. Overall detection efficiency is very high owing to the nearly 100% detection efficiency of the Si detectors of the CHIMERA system. However, we want to know the extent to which various distributions, characterizing dynamical and equilibrium fission, are affected by the configuration of the instrument. This is determined not only by efficiency but also by resolution effects. For

example, the recorded in-plane angular distribution can be disturbed not only by the smaller detection efficiency at some regions of angles but also because the angular resolution can result in shifting the counts from one angle to another. As a consequence, if we define the “detection efficiency” as the ratio of the number of events measured in some angular intervals to the true number of events in the same intervals (or the ratio of the number of events at the output and input of the detector system), we can observe that the efficiency defined in this way can be smaller or larger than 100%.

The efficiency of CHIMERA depends on the velocity vectors of both fission fragments. Physically, these are defined by the fissioning nucleus velocity, its deflection angle during collision with the target, the mass asymmetry of fission, the angular distributions, and the fragment relative velocity.

Since we are able to present at most 3-dim distributions, we have to integrate over the other quantities. Here physics comes into play, as it defines the distributions of these quantities. To calculate the instrument angular response function we

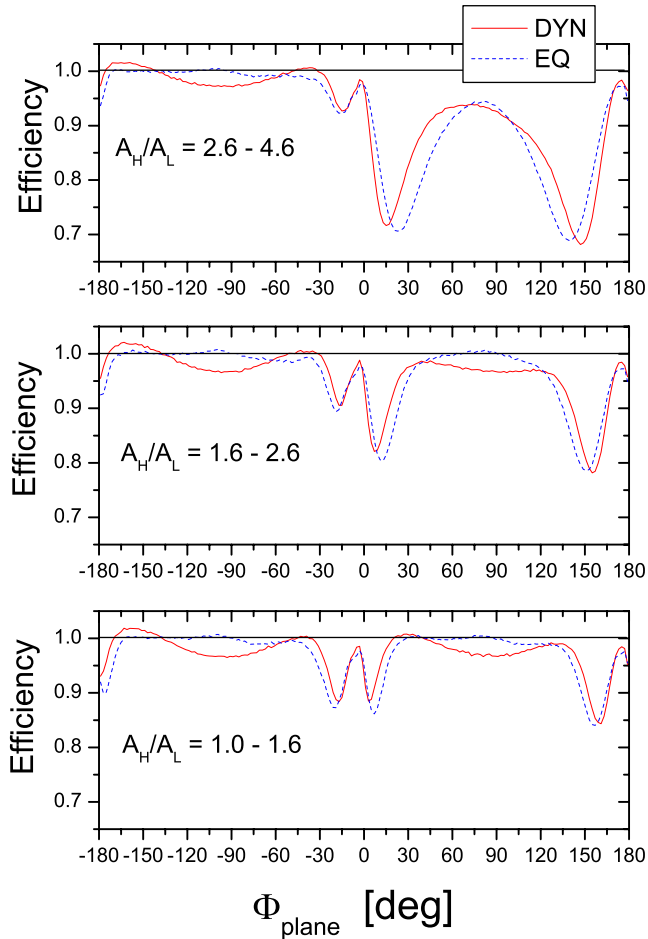


FIG. 9. (Color online) CHIMERA detection efficiency as a function of the in-plane angle for equilibrated and dynamical fissions, calculated for three mass asymmetry intervals.

performed Monte Carlo simulation of the detection efficiency trying as much as possible to use the experimental (even if approximate) information. Unfortunately, we do not know

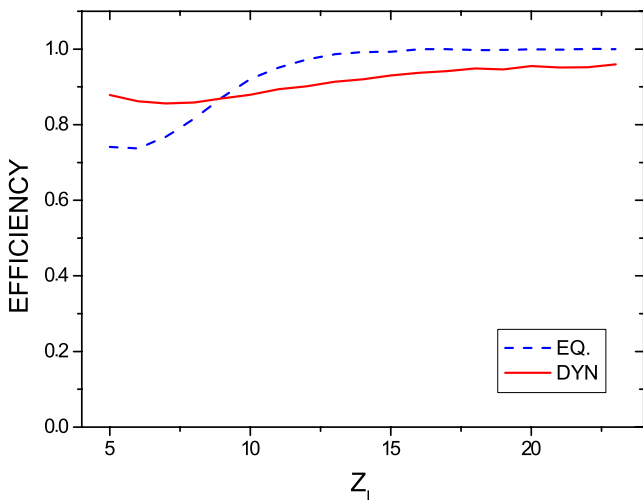


FIG. 10. (Color online) The  $Z_L$  dependence of detection efficiency calculated for equilibrated and dynamical fission.

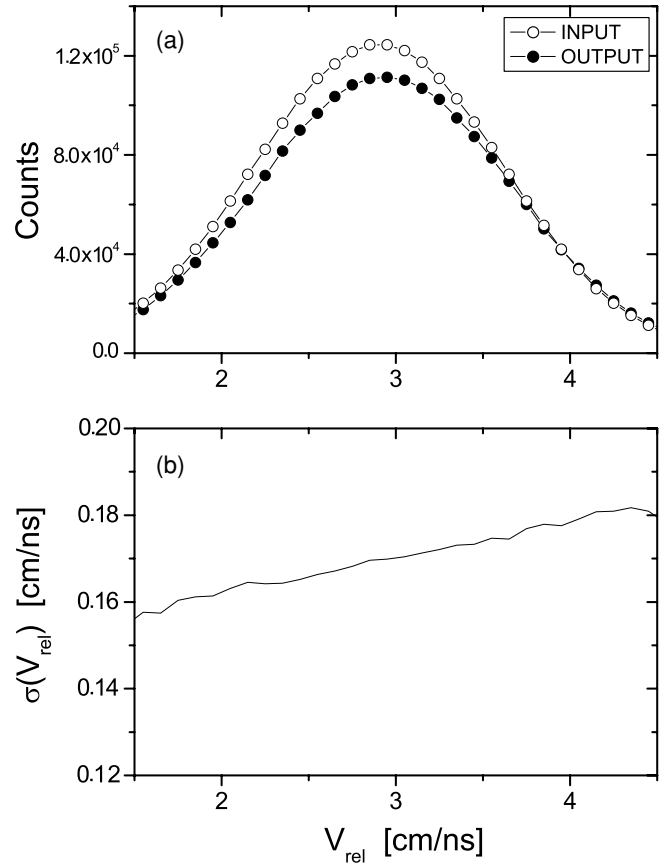


FIG. 11. (a) Comparison of the relative velocity spectrum at the input and output of the detection system. (b) Resolution of  $V_{\text{rel}}$  caused by the position resolution of the CHIMERA system.

the possible correlations between various quantities, so in most cases we have to assume that they are not correlated. However, we performed our simulations by taking into account the observed differences between dynamical and equilibrated processes. This concerns in particular distributions of the mass asymmetry, out-of plane angles, and relative velocities (see Fig. 8.)

Integrating over the out-of-plane angular distributions and dividing the output by input distributions, we obtained the “efficiency” of  $\Phi_{\text{plane}}$  distribution measurements for equilibrated and dynamical fission (see Fig. 9). Note that an efficiency  $>1.0$  is caused by the aforementioned resolution effects: According to simulations for  $\Phi_{\text{plane}}$  it amounts (in terms of rms) to  $4\text{--}5^\circ$  in the dynamical component and  $5\text{--}8^\circ$  in the equilibrated component (depending on  $\Phi_{\text{plane}}$ ). For  $\Psi_{\text{out}}$ , the resolution equals  $7\text{--}9^\circ$  for both components. To a large extent the finite resolution is caused by the small scattering angle of the studied system, which gives rise to the poor reaction plane determination.

The conclusion of the simulations is that depletion in the  $\Phi_{\text{plane}}$  distribution (Fig. 9), seen in our experimental results close to  $\pm 15^\circ$ , is caused by a 10–30% reduction in efficiency, caused by the beam exit hole in the CHIMERA system.

Next, we checked to what extent the fragment charge distribution can be disturbed by detection efficiency effects. The results, shown in Fig. 10, prove that the effect, although present, can be safely neglected, both for EQ and DYN components, if one takes into account the exponential dependence of the charge distributions for small  $Z_L$  values.

Also, the influence of geometric imperfections of CHIMERA on the fragments' relative velocity is expected to be very weak. This is illustrated in Fig. 11, where one can compare the (simulated) "true" and measured relative velocity

spectra for the DF process. It is seen that despite some energy shift between both distributions, the effect is weak and regular. This means that irregularities observed in the experimental Viola ratio distributions [Fig. 7(a)] are generated by other means. They are, in fact, caused by using a rather rough way of selecting the DF events, namely, by putting the condition on  $V_{\text{par}}^L$ .

The resolution of  $V_{\text{rel}}$  measurements, limited by the position resolution of the CHIMERA detectors, being of the order of 0.17 cm/ns, is, for the purpose of this study, quite satisfactory.

- 
- [1] P. Glassel, D. von Harrach, and H. J. Specht, *Z. Phys. A* **310**, 189 (1983).
- [2] A. A. Stefanini *et al.*, *Z. Phys. A* **351**, 167 (1995).
- [3] F. Bocage *et al.*, *Nucl. Phys. A* **676**, 391 (2000).
- [4] J. Colin *et al.*, *Phys. Rev. C* **67**, 064603 (2003).
- [5] G. Poggi, *Nucl. Phys. A* **685**, 296c (2001).
- [6] J. Lukasik *et al.*, *Phys. Rev. C* **55**, 1906 (1997).
- [7] V. Baran, M. Colonna, and M. Di Toro, *Nucl. Phys. A* **730**, 329 (2004).
- [8] A. Pagano *et al.*, *Nucl. Phys. A* **681**, 331c (2001).
- [9] E. Geraci *et al.*, *Nucl. Phys. A* **732**, 173 (2004); S. Aiello *et al.*, *Nucl. Instrum. Methods A* **369**, 50 (1996); S. Aiello *et al.*, *ibid.* **385**, 306 (1997); S. Aiello *et al.*, *IEEE Trans. Nucl. Sci.* **45**, 4, 1877 (1998); S. Aiello *et al.*, *Nucl. Instrum. Methods A* **427**, 510 (1999); N. Le Neindre *et al.*, *ibid.* **490**, 251 (2002); M. Alderighi *et al.*, *ibid.* **489**, 257 (2002).
- [10] W. F. W. Schneider *et al.*, *Nucl. Instrum. Methods* **87**, 253 (1970).
- [11] A. Pagano *et al.*, in *Proceedings of the XLII International Winter Meeting on Nuclear Physics, Bormio (Italy), 25–31 Jan. 2004*, edited by I. Iori (Ricerca Scientifica ed Educazione Permanente, University of Milan, 2004), Suppl. 123.
- [12] A. Pagano *et al.*, *Nucl. Phys. A* **734**, 504 (2004).
- [13] J. Wilczyński *et al.*, *Int. J. Mod. Phys.* **14**, 353 (2005), in press; E. De Filippo *et al.*, *Phys. Rev. C* **71**, 044602 (2005).
- [14] R. Vandenbosh and J. R. Huizenga, *Nuclear Fission* (Academic Press, New York, 1973).
- [15] J. C. Steckmeyer, F. Lefebvres, C. Le Brun, J. F. Lecolley, M. L'Haridon, A. Osmont, and J. P. Patry, *Nucl. Phys. A* **427**, 357 (1984).
- [16] D. Hilscher and H. Rossner, *Ann. Phys. (Paris)* **17**, 471 (1992).
- [17] P. Staszal, Z. Majka, L. G. Sobotka, V. Abenante, N. G. Nicolis, D. G. Sarantites, D. W. Stracener, C. Baktash, M. L. Halbert, and D. C. Hensley, *Phys. Lett.* **B368**, 26 (1996).
- [18] F. Goldenbaum *et al.*, *Phys. Rev. Lett.* **82**, 5012 (1999).
- [19] D. J. Hinde, J. R. Leigh, J. J. M. Bokhorst, J. O. Newton, R. L. Walsh, and J. W. Boldeman, *Nucl. Phys. A* **472**, 318 (1987).
- [20] D. Vorkapic and B. Ivanisevic, *Phys. Rev. C* **52**, 1980 (1995); Z. Liu, H. Zhang, J. Xu, Y. Qiao, X. Qian, and C. Lin, *Phys. Lett.* **B353**, 173 (1995).